Copper-Mediated Radiosynthesis of [^{18}F]Rucaparib

Zijun Chen,[a] Gianluca Destro,[a,b] Florian Guibbal,[a,b] Chung Ying Chan,[b] Bart Cornelissen,[b] and Véronique Gouverneur[a,*]

[a]Chemistry Research Laboratory, Oxford University, Oxford OX1 3TA, U.K.

[b]MRC Oxford Institute for Radiation Oncology, Department of Oncology, University of Oxford, Oxford, OX3 7LJ, U.K.

Supporting Information Placeholder

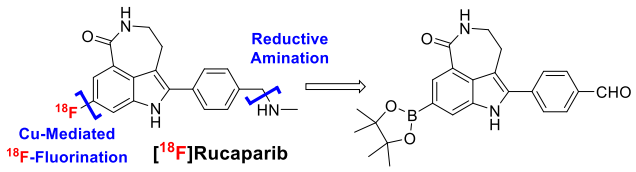

ABSTRACT: The poly(ADP-ribose) polymerase (PARP) inhibitor rucaparib is used in the clinic to treat *BRCA*-mutated cancers. Herein, we report two strategies to access the ^{18}F-isotopologue of rucaparib applying a copper-mediated nucleophilic ^{18}F-fluorodeboronation. The most successful approach features an aldehydic boronic ester precursor subjected to reductive amination post ^{18}F-labeling and affords [^{18}F]rucaparib with an activity yield of 11% ± 3% (n = 3), and molar activity (A_m) up to 30 GBq/μmol. Preliminary *in vitro* studies are presented.

Poly(ADP-ribose) polymerase (PARP) inhibitors, a class of cancer drugs exploiting synthetic lethality, have demonstrated promising results in the treatment of various cancers with *BRAC1/2* mutation.[1] Four PARP inhibitors are FDA-approved for clinical use, including olaparib (Lynparza, AstraZeneca), rucaparib (Rubraca, Clovis Oncology), niraparib (Zejula, Tesaro, Inc.), and talazoparib (Talzenna, Pfizer).[1] For some patients, poor response to treatment with PARP inhibitors is observed, which may be caused by a lack of drug accumulation in the tumor, active drug efflux, or other resistance mechanisms.[2,3,4,5] Therefore, a method that estimates PARP expression levels, PARP inhibitor accumulation in tumor tissue, and/or target occupancy of PARP enzyme binding pockets, may allow more accurate selection or fast therapy evaluation of patients who may benefit from PARP inhibitor treatment. Tritium-labeled rucaparib is suitable for *ex vivo* autoradiographic or liquid scintillation quantification (Scheme 1A), and [$^{123/125}$I]KX-1, is a structurally related radiotracer that can measure PARP-1 expression *in vitro* and *in vivo* (Scheme 1B).[6,7] In this context, positron emission tomography (PET) imaging stands out for clinical standard of care because this technique could enable quantification of PARP expression in cancerous tissue in patients using radiolabeled PARP inhibitors.[8,9] As a radioisotope, fluorine-18 is ideal because of its half-life of 109.8 minutes, relatively low energy and abundant positron emission profile. With these considerations in mind, radiotracers that have structural similarities with rucaparib have been studied. The radiotracer [^{18}F]WC-DZ-F was applied for the preliminary evaluation of PARP expression in prostate cancer, and [^{18}F]FluorThanatrace developed by Mach *et al.* is being evaluated as a PET imaging agent for clinical use (Scheme 1B).[10,11] Other examples include [^{18}F]PARPi, with a first-in-man study in head-and-neck cancer patients recently reported.[12]

Scheme 1. Labeled PARP inhibitors and analogues

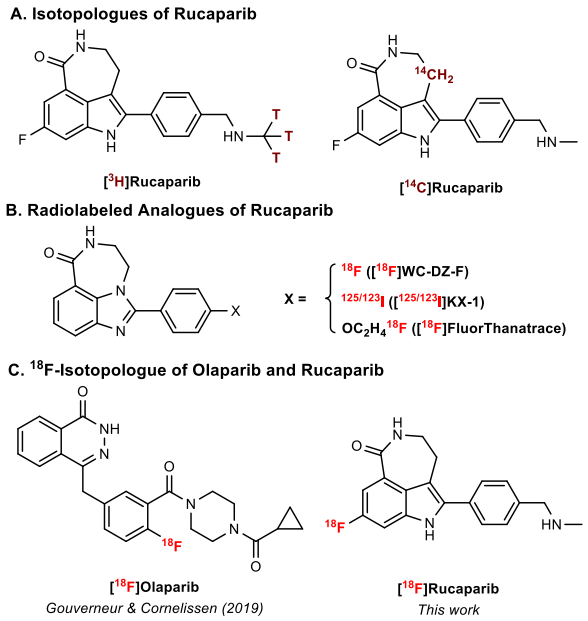

Using structurally identical ^{18}F-isotopologues of PARP inhibitors presents several advantages as these allow direct visualization of PARP expression in patients with PET imaging, as well as enable quantification of PARP inhibitor biodistribution, tumor delivery and target engagement; as such

stratification of patients becomes possible and response to DNA damaging cancer treatment can be monitored.[13] [^{3}H]rucaparib and [^{14}C]rucaparib were prepared to study metabolism using *ex vivo* autoradiography and radio-HPLC (Scheme 1A),[6,14] but to the best of our knowledge, [^{18}F]rucaparib has not been synthesized and studied to date (Scheme 1C). As part of our ongoing program focused on the evaluation of radiolabeled PARP inhibitors, we recently reported the radiosynthesis of [^{18}F]olaparib and demonstrated that this radiotracer is taken up in PARP-1 expressing cell lines and tumor in xenografted mice, with increased uptake upon tumor irradiation.[15,16] Herein, we disclose the first radiosynthesis of [^{18}F]rucaparib featuring as key step a Cu-mediated radiofluorination of an aryl boronic ester with cyclotron-produced ^{18}F-fluoride, a labeling reaction invented in our laboratory.[17,18,19] Initial *in vitro* studies are also presented.

Late stage or last step ^{18}F-incorporation is ideal due to the short half-life of the radionuclide, but such strategy often carries risk especially for functionalized ^{18}F-radiotracers containing one or more *N*-heterocycles. We recently reported a robustness screening approach to determine whether ^{18}F-fluorodeboronation as the last step in the synthesis is viable.[19] If not possible, this screening approach also enables to decide which step(s) should follow ^{18}F-fluorination. In practice, a model aryl boronic ester responding well to ^{18}F-labeling, such as 2-(4-cyanophenyl)-4,4,5,5-tetramethyl-1,3,2-dioxaborolane (radiochemical yield (RCY) = 39% ± 2%, *n* = 4), is subjected to Cu-mediated ^{18}F-fluorodeboronation in the presence of stoichiometric amounts of the molecule to be labeled, or a close structural analogue. If the presence of this additive does not affect the RCY, a last step ^{18}F-fluorination is likely viable. However, if the RCY is markedly decreased, or no ^{18}F-incorporation is observed (RCY < 5%), it is necessary to identify which group or sub-motif affects detrimentally ^{18}F-radiofluorination. This group must be introduced post ^{18}F-labeling, or may require protection prior to ^{18}F-labeling. Following this workflow, a model boronic ester was subjected to Cu-mediated ^{18}F-fluorination in the presence of a stoichiometric amount of the non-fluorinated analogue of rucaparib **1**; under these conditions, only a trace amount of [^{18}F]4-fluorobenzonitrile was observed. This experiment discouraged ^{18}F-incorporation as the last step (Scheme 2).

Scheme 2. Robustness screening experiments informing suitable radiosynthetic routes towards [^{18}F]rucaparib

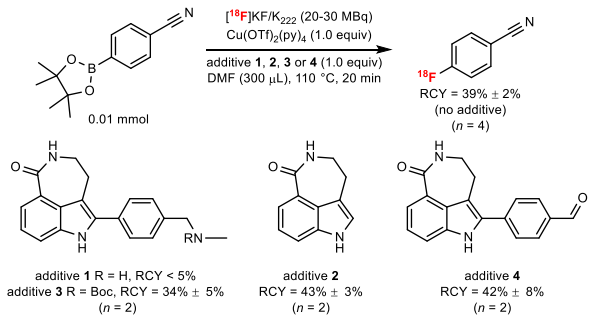

Upon spiking with the tricyclic indole **2**, the RCY for the benchmark reaction was not affected (~ 43%), a result indicating that the secondary amine prevented ^{18}F-fluorination. Thus, we envisaged two strategies to overcome this limitation consisting of post-radiolabeling deprotection of an NBoc protected precursor[19] or reductive amination, the latter option being inspired by the synthesis of rucaparib.[20] We were indeed encouraged by the finding that spiking the model reaction with carbamate **3** (RCY = 34% ± 5%, *n* = 2) or aldehyde **4** (RCY = 42% ± 8%, *n* = 2), did not affect the RCY of [^{18}F]4-fluorobenzonitrile. These results boded well for a two-step radiosynthesis consisting of a copper-mediated ^{18}F-fluorodeboronation followed by either NBoc deprotection or reductive amination.

Scheme 3. Synthesis of the NBoc protected or aldehydic aryl boronic ester precursors 12 and 14 required for ^{18}F-radiolabeling

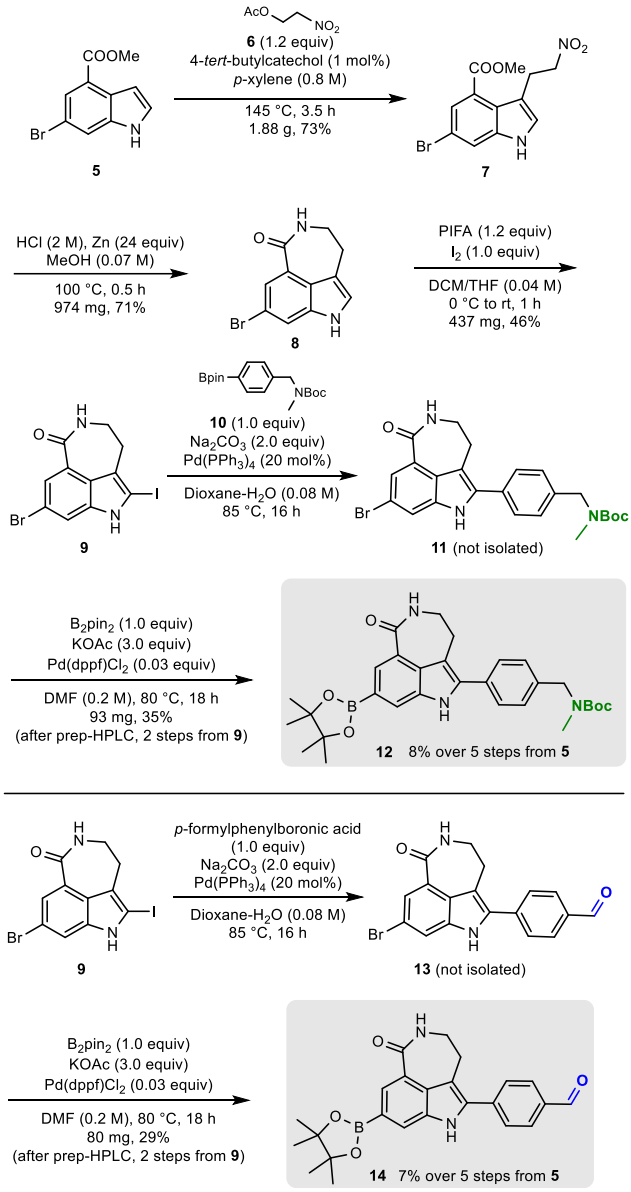

On the basis of these experiments, efforts focused on the multi-step synthesis of the borylated rucaparib precursors **12** and **14** (Scheme 3). Both precursors were made accessible from the novel *bis*-halogenated tricyclic indole **9** by modifying a sequence disclosed in the literature (Scheme 3).[20,21] The synthesis started with the reaction of commercially available methyl 6-bromo-4-indolecarboxylate **5** with 2-nitroethylacetate **6**, made available by esterification of nitroethanol,[22] to afford (2-nitroethyl)indole **7** which is required for ring closure. Upon reduction with zinc in methanolic hydrochloric acid, lactonization led to the tricyclic indole **8** in 71% yield. Regioselective iodination at the C2-indole with PIFA/I_2 (PIFA = [bis(trifluoroacetoxy)iodo]benzene) took place within an hour and led to the *bis*-halogenated **9** in 46% yield. Chemoselective Suzuki-Miyaura reaction enabled further functionalization. Coupling with the *N*-protected boronic ester **10**[22] furnished the brominated carbamate **11**, which was immediately subjected to borylative coupling to afford the desired boronic ester **12**. After preparative HPLC purification, **12** required for ^{18}F-incorporation was obtained with an overall yield of 8% (chemical purity > 95%) from commercially available indole **5**. Similarly, coupling between **9** and *p*-formylphenyl boronic acid followed by a borylative coupling led to the *N*-protected boronic ester **14** with an overall yield of 7% (chemical purity > 95%) from commercially available indole **5** (Scheme 3).

Table 1. Optimization study for the ^{18}F-radiolabeling of the *N*-protected boronic ester precursor 12

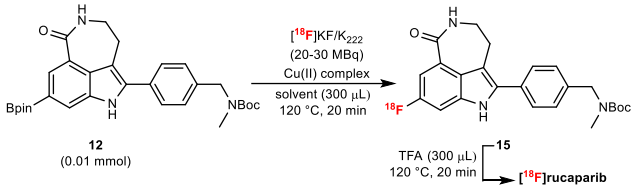

Entry	Solvent	$Cu(OTf)_2(py)_4$	RCY[a]
1	**DMI**	**1 equiv**	**42%**
2	DMI	2 equiv	39%
3	DMI	3 equiv	25%
4	DMF	2 equiv	7%
5	DMI	2 equiv[b]	1%

[a]RCY = radiochemical yield, determined by analytical HPLC. [b]Reaction performed with the copper complex $Cu(OTf)_2(impy)_4$. K_{222} = 4,7,13,16,21,24-hexaoxa-1,10-diazabicyclo[8.8.8]hexacosane or Kryptofix 222. DMI = 1,3-dimethyl-2-imidazolidinone. DMF = *N*,*N*-dimethylformamide.

Studies on the radiofluorination of **12** and **14** were undertaken next. The labeling of the NBoc protected precursor **12** with [^{18}F]KF was carried out in the presence of $Cu(OTf)_2(py)_4$ in DMI at 120 °C for 20 minutes affording [^{18}F]**15** in 42% RCY (Table 1, entry 1). For this process, elution was performed with a solution of $K_{222}/K_2C_2O_4/K_2CO_3$.[22] Slight modification of these labeling conditions did not improve the RCY (Table 1, entry 2-5). Deprotection of [^{18}F]**15** with TFA at 120 °C for 20 minutes was quantitative. When the aldehydic precursor **14** was subjected to the reaction condition found optimal for **12**, the RCY of [^{18}F]**16** was significantly higher (73% RCY, Table 2, entry 1). Further optimization by modifying the stoichiometry of the copper complex with respect to the boronic ester precursor, the solvent and the nature of the copper complex by replacing $Cu(OTf)_2(py)_4$ with $Cu(OTf)_2(impy)_4$ (impy = imidazo[1,2-*b*]pyridazine)[15] indicated that the best result was obtained by increasing the $Cu(OTf)_2(py)_4$:**14** ratio from 1:1 to 2:1. These ^{18}F-labeling conditions gave [^{18}F]**16** in 80% RCY (Table 2, entries 2–5).

Table 2. Optimization study for the ^{18}F-radiolabeling of the aldehydic boronic ester precursor 14

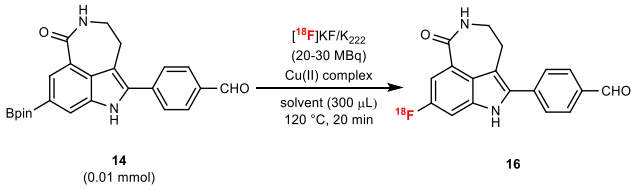

Entry	Solvent	$Cu(OTf)_2(py)_4$	RCY[a]
1	DMI	1 equiv	73%
2	**DMI**	**2 equiv**	**80%**
3	DMI	3 equiv	56%
4	DMF	2 equiv	13%
5	DMI	2 equiv[b]	14%

[a]RCY = radiochemical yield, determined by analytical HPLC. [b]Reaction performed with the copper complex $Cu(OTf)_2(impy)_4$.

We subjected **14** to a one-pot ^{18}F-radiofluorination followed by reductive amination, the latter step being carried out in the presence of methylamine and $NaBH_3CN$ in EtOH for 20 minutes at 120 °C. Reductive amination was quantitative as determined by radio-HPLC. The identity of [^{18}F]rucaparib was confirmed by analytical radio-HPLC showing overlap of the radio- and the UV chromatogram of unlabeled rucaparib (220 nm). This result led us to select this radiosynthetic route for the synthesis of [^{18}F]rucaparib. Starting from 2 to 3 GBq of [^{18}F]fluoride, this semi-automated protocol afforded [^{18}F]rucaparib isolated and reformulated in 10% DMSO/PBS solution with a non-decay corrected activity yield (AY) of 11% ± 3% (n = 3), a radiochemical purity (RCP) superior to 95%, and molar activity (A_m) up to 30 GBq/µmol; the total synthesis time was 2.5 h (Figure 1).[22]

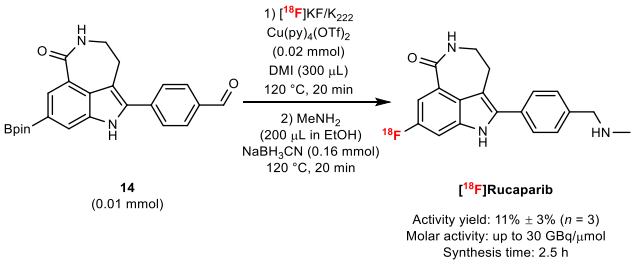

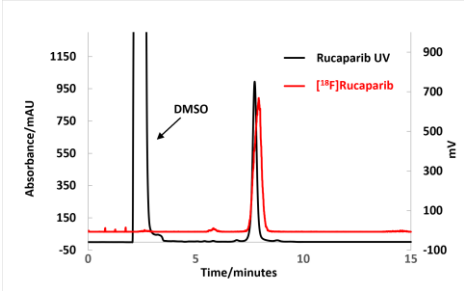

Figure 1. Radiochromatogram secured by HPLC analysis of [18F]rucaparib (red) overlayed with UV chromatogram of non-radiolabeled rucaparib (l = 220 nm) (black).

In vitro studies revealed the uptake of [18F]rucaparib in human pancreatic adenocarcinoma (PDAC) cells, AsPC1 and PSN1. PSN1 cells, inherently expressing higher PARP1 level than AsPC1 cells,[23] retained [18F]rucaparib more effectively, indicating correlation between rucaparib uptake and PARP1 expression (Figure 2A). The binding specificity of [18F]rucaparib was assessed by blocking studies using non-radiolabeled PARP inhibitor.[24] Addition of an excess (> 1000 fold) of olaparib or rucaparib significantly reduced (> 50%) [18F]rucaparib uptake in PSN1 cells, a safe indicator of selective binding (Figure 2B).

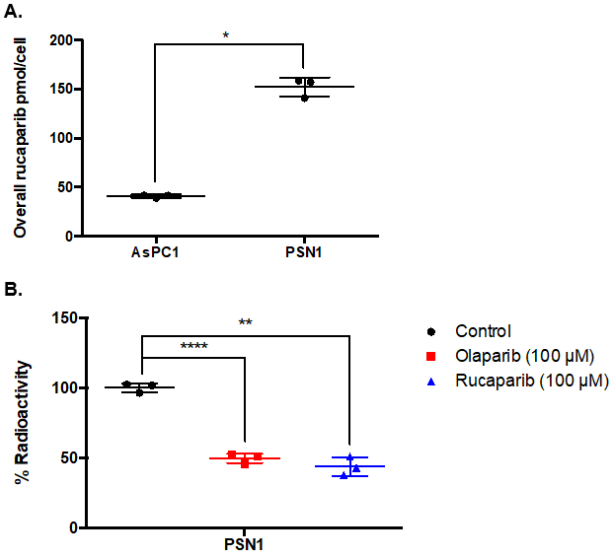

Figure 2. A. Rucaparib uptake in AsPC1 and PSN1 cells. Asterisks indicate levels of significance: *, P < 0.05. **B.** Blocking of [18F]rucaparib uptake in PSN1 cells by addition of an excess of non-labeled olaparib or rucaparib. Asterisks indicate levels of significance: **, P < 0.01; and ****, P < 0.0001.

In summary, the first radiosynthesis of the 18F-radioisotopologue of rucaparib is disclosed. Two strategies were examined based on the results of a preliminary robustness screening study. The optimal strategy is a two-step protocol consisting of a Cu(II)-mediated 18F-fluorodeboronation followed by quantitative reductive amination, which provides [18F]rucaparib in good AY and RCP. Our preliminary *in vitro* studies show specific uptake of [18F]rucaparib in human PDAC cell lines, indicating the potential of [18F]rucaparib as a PARP-targeting PET imaging agent. Additional evaluation of [18F]rucaparib are warranted to define its possible uses.

ASSOCIATED CONTENT

Supporting Information

The Supporting Information is available free of charge on the ACS Publications website.

Experimental data, characterization data, 18F-radiotraces (PDF)

AUTHOR INFORMATION

Corresponding Author

Véronique Gouverneur – *Chemistry Research Laboratory, Oxford University, Oxford OX1 3TA, U.K.;* orcid.org/ 0000-0001-8638-5308; Email: veronique.gouverneur@ chem.ox.ac.uk

Notes

The authors declare no competing financial interest.

ACKNOWLEDGMENT

We acknowledge financial support from Cancer Research UK through the Oxford Institute for Radiation Oncology, Medical Research Council (MRC) (MR/R01695X/1, G.D. and F.G.) and Pancreatic Cancer UK (PCUK H3R00510, C.Y.C).

REFERENCES

(1) Lord, C. J.; Ashworth, A., PARP inhibitors: Synthetic lethality in the clinic. *Science* **2017**, *355* (6330), 1152–1158.

(2) Livraghi, L.; Garber, J. E., PARP Inhibitors in the Management of Breast Cancer: Current Data and Future Prospects. *BMC Med.* **2015**, *13*, 188.

(3) Kim, Y.; Kim, A.; Sharip, A.; Sharip, A.; Jiang, J.; Yang, Q.; Xie, Y., Reverse the Resistance to PARP Inhibitors. *Int. J. Biol. Sci.* **2017**, *13* (2), 198–208.

(4) Walsh, N.; Larkin, A.; Kennedy, S.; Connolly, L.; Ballot, J.; Ooi, W.; Gullo, G.; Crown, J.; Clynes, M.; O'Driscoll, L., Expression of Multidrug Resistance Markers ABCB1 (MDR-1/P-gp) and ABCC1 (MRP-1) in Renal Cell Carcinoma. *BMC Urology* **2009**, *9* (1), 6.

(5) Li, H.; Liu, Z.-Y.; Wu, N.; Chen, Y.-C.; Cheng, Q.; Wang, J., PARP Inhibitor Resistance: the Underlying Mechanisms and Clinical Implications. *Mol. Cancer* **2020**, *19* (1), 107.

(6) Alluri, S. R.; Riss, P. J., Poly(ADP-ribose) Polymerase in Neurodegeneration: Radiosynthesis and Radioligand Binding in ARC-SWE tg Mice. *ACS Chem. Neurosci.* **2018**, *9* (6), 1259–1263.

(7) (a) Makvandi, M.; Xu, K.; Lieberman, B. P.; Anderson, R.-C.; Effron, S. S.; Winters, H. D.; Zeng, C.; McDonald, E. S.; Pryma, D. A.; Greenberg, R. A.; Mach, R. H., A Radiotracer Strategy to Quantify PARP-1 Expression *In Vivo* Provides a Biomarker That Can Enable Patient Selection for PARP Inhibitor Therapy. *Cancer Res.* **2016**, *76* (15),1–9. (b) Riad, A.; Gitto, S. B.; Lee, H.; Winters, H. D.; Martorano, P. M.; Hsieh, C.-J.; Xu, K.; Omran, D. K.; Powell, D. J.; Mach, R. H.; Makvandi, M., PARP Theranostic Auger Emitters Are Cytotoxic in BRCA Mutant Ovarian Cancer and Viable Tumors from

Ovarian Cancer Patients Enable Ex-Vivo Screening of Tumor Response. *Molecules* **2020**, *25* (24), 6029. (c) For radiolabeled rucaparib solely used for therapeutic purpose, see [^{211}At]MM4: Makvandi, M.; Lee, H.; Puentes, L. N.; Reilly, S. W.; Rathi, K. S.; Weng, C.-C.; Chan, H. S.; Hou, C.; Raman, P.; Martinez, D.; Xu, K.; Carlin, S. D.; Greenberg, R. A.; Pawel, B. R.; Mach, R. H.; Maris, J. M.; Pryma, D. A., Targeting PARP-1 with Alpha-Particles Is Potently Cytotoxic to Human Neuroblastoma in Preclinical Models. *Mol. Cancer Ther.* **2019**, *18* (7), 1195–1204.

(8) Phelps, M. E., Positron Emission Tomography Provides Molecular Imaging of Biological Processes. *Proc. Natl Acad. Sci.* **2000**, *97* (16), 9226–9233.

(9) Miller, P. W.; Long, N. J.; Vilar, R.; Gee, A. D., Synthesis of ^{11}C, ^{18}F, ^{15}O, and ^{13}N Radiolabels for Positron Emission Tomography. *Angew. Chem. Int. Ed.* **2008**, *47* (47), 8998–9033.

(10) Zhou, D.; Xu, J.; Mpoy, C.; Chu, W.; Kim, S. H.; Li, H.; Rogers, B. E.; Katzenellenbogen, J. A., Preliminary Evaluation of a Novel ^{18}F-Labeled PARP-1 Ligand for PET Imaging of PARP-1 Expression in Prostate Cancer. *Nucl. Med. Biol.* **2018**, *66*, 26–31.

(11) (a) Zhou, D.; Chu, W.; Xu, J.; Jones, L. A.; Peng, X.; Li, S.; Chen, D. L.; Mach, R. H., Synthesis, [^{18}F]Radiolabeling, and Evaluation of Poly(ADP-ribose) Polymerase-1 (PARP-1) Inhibitors for *In Vivo* Imaging of PARP-1 Using Positron Emission Tomography. *Bioorg. Med. Chem.* **2014**, *22* (5), 1700–1707. (b) Edmonds, C. E.; Makvandi, M.; Lieberman, B. P.; Xu, K.; Zeng, C.; Li, S.; Hou, C.; Lee, H.; Greenberg, R. A.; Mankoff, D. A.; Mach, R. H., [^{18}F]FluorThanatrace Uptake as a Marker of PARP1 Expression and Activity in Breast Cancer. *Am. J. Nucl. Med. Mol. Imaging* **2016**, *6* (1), 94–101. (c) Chen, D.; Dyroff, S.; Michel, L.; Wang-Gillam, A.; Tan, B.; Phillips, S.; Bognar, C.; Chu, W.; Zhou, D.; Mach, R.; Brooks, F.; Laforest, R., First-in-human Studies Characterizing a Poly(ADP-ribose) Polymerase (PARP) Targeted Tracer, ^{18}F-FluorThanatrace (^{18}F-FTT) for Cancer Imaging. *J. Nucl. Med.* **2016**, *57* (supplement 2), 582. (d) Pantel, A.; MaKvandi, M.; Doot, R.; Schwartz, L.; Greenberg, R.; Simpkins, F.; Mankoff, D.; Lin, L.; Mach, R., A Pilot Study of a Novel Poly(ADP-ribose) Polymerase-1 (PARP) PET Tracer ([^{18}F]FluorThanatrace) in Patients with Ovarian Carcinoma. *J. Nucl. Med.* **2017**, *58* (supplement 1), 386. (e) Makvandi, M.; Pantel, A.; Schwartz, L.; Schubert, E.; Xu, K.; Hsieh, C.-J.; Hou, C.; Kim, H.; Weng, C.-C.; Winters, H.; Doot, R.; Farwell, M. D.; Pryma, D. A.; Greenberg, R. A.; Mankoff, D. A.; Simpkins, F.; Mach, R. H.; Lin, L. L., A PET Imaging Agent for Evaluating PARP-1 Expression in Ovarian Cancer. *J. Clin. Invest.* **2018**, *128* (5), 2116–2126.

(12) Schöder, H.; França, P. D. D. S.; Nakajima, R.; Burnazi, E.; Roberts, S.; Brand, C.; Grkovski, M.; Mauguen, A.; Dunphy, M. P.; Ghossein, R. A.; Lyashchenko, S. K.; Lewis, J. S.; Donoghue, J. A.; Ganly, I.; Patel, S. G.; Lee, N. Y.; Reiner, T., Safety and Feasibility of PARP1/2 Imaging with ^{18}F-PARPi in Patients with Head and Neck Cancer. *Clin. Cancer Res.* **2020**, *26* (13), 3110–3116.

(13) Chan, C. Y.; Tan, K. V.; Cornelissen, B., PARP Inhibitors in Cancer Diagnosis and Therapy. *Clin. Cancer Res.* **2021**, *27* (6), 1585–1594.

(14) Liao, M.; Watkins, S.; Nash, E.; Isaacson, J.; Etter, J.; Beltman, J.; Fan, R.; Shen, L.; Mutlib, A.; Kemeny, V.; Pápai, Z.; van Tilburg, P.; Xiao, J. J., Evaluation of Absorption, Distribution, Metabolism, and Excretion of [^{14}C]Rucaparib, a Poly(ADP-ribose) Polymerase Inhibitor, in Patients with Advanced Solid Tumors. *Invest. New Drugs* **2020**, *38* (3), 765–775.

(15) Wilson, T. C.; Xavier, M.-A.; Knight, J.; Verhoog, S.; Torres, J. B.; Mosley, M.; Hopkins, S. L.; Wallington, S.; Allen, P. D.; Kersemans, V.; Hueting, R.; Smart, S.; Gouverneur, V.; Cornelissen, B., PET Imaging of PARP Expression Using [^{18}F]Olaparib. *J. Nucl. Med.* **2019**, *60* (4), 504–510.

(16) Guibbal, F.; Isenegger, P. G.; Wilson, T. C.; Pacelli, A.; Mahaut, D.; Sap, J. B. I.; Taylor, N. J.; Verhoog, S.; Preshlock, S.; Hueting, R.; Cornelissen, B.; Gouverneur, V., Manual and Automated Cu-Mediated Radiosynthesis of the PARP Inhibitor [^{18}F]Olaparib. *Nat. Protoc.* **2020**, *15* (4), 1525–1541.

(17) Tredwell, M.; Preshlock, S. M.; Taylor, N. J.; Gruber, S.; Huiban, M.; Passchier, J.; Mercier, J.; Génicot, C.; Gouverneur, V., A General Copper-Mediated Nucleophilic ^{18}F-Fluorination of Arenes. *Angew. Chem. Int. Ed.* **2014**, *53* (30), 7751–7755.

(18) Preshlock, S.; Calderwood, S.; Verhoog, S.; Tredwell, M.; Huiban, M.; Hienzsch, A.; Gruber, S.; Wilson, T. C.; Taylor, N. J.; Cailly, T.; Schedler, M.; Collier, T. L.; Passchier, J.; Smits, R.; Mollitor, J.; Hoepping, A.; Mueller, M.; Genicot, C.; Mercier, J.; Gouverneur, V., Enhanced Copper-mediated ^{18}F-Fluorination of Aryl Boronic Esters Provides Eight Radiotracers for PET Applications. *Chem. Commun.* **2016**, *52* (54), 8361–8364.

(19) Taylor, N. J.; Emer, E.; Preshlock, S.; Schedler, M.; Tredwell, M.; Verhoog, S.; Mercier, J.; Genicot, C.; Gouverneur, V., Derisking the Cu-Mediated ^{18}F-Fluorination of Heterocyclic Positron Emission Tomography Radioligands. *J. Am. Chem. Soc.* **2017**, *139* (24), 8267–8276.

(20) Webber S. E.; Canan-Koch S. S.; Tikhe J. G.; Thoresen L. H., Tricyclic Inhibitors of Poly(ADP-ribose) Polymerases. U. S. Patent WO 2000042040A1, July 20, 2000.

(21) Canan Koch, S. S.; Thoresen, L. H.; Tikhe, J. G.; Maegley, K. A.; Almassy, R. J.; Li, J.; Yu, X.-H.; Zook, S. E.; Kumpf, R. A.; Zhang, C.; Boritzki, T. J.; Mansour, R. N.; Zhang, K. E.; Ekker, A.; Calabrese, C. R.; Curtin, N. J.; Kyle, S.; Thomas, H. D.; Wang, L.-Z.; Calvert, A. H.; Golding, B. T.; Griffin, R. J.; Newell, D. R.; Webber, S. E.; Hostomsky, Z., Novel Tricyclic Poly(ADP-ribose) Polymerase-1 Inhibitors with Potent Anticancer Chemopotentiating Activity: Design, Synthesis, and X-ray Cocrystal Structure. *J. Med. Chem.* **2002**, *45* (23), 4961–4974.

(22) See Supporting Information for more details.

(23) Guibbal, F.; Hopkins, S. L.; Pacelli, A.; Isenegger, P. G.; Mosley, M.; Torres, J. B.; Dias, G. M.; Mahaut, D.; Hueting, R.; Gouverneur, V.; Cornelissen, B., [^{18}F]AZD2461, an Insight on Difference in PARP Binding Profiles for DNA Damage Response PET Imaging. *Mol. Imaging Biol.* **2020**, *22* (5), 1226–1234.

(24) Carney, B.; Kossatz, S.; Lok, B. H.; Schneeberger, V.; Gangangari, K. K.; Pillarsetty, N. V. K.; Weber, W. A.; Rudin, C. M.; Poirier, J. T.; Reiner, T., Target Engagement Imaging of PARP Inhibitors in Small-Cell Lung Cancer. *Nat. Commun.* **2018**, *9* (1), 176.